

## Experimental Determination of Mechanical Properties of Banana Jute Hybrid Composite

B. Vijaya Ramnath\*, R. Sharavanan<sup>1</sup>, M. Chandrasekaran<sup>2</sup>, C. Elanchezhian, R. Sathyanarayanan,  
R. Niranjan Raja, and S. Junaid Kokan

Department of Mechanical Engineering, Sri Sairam Engineering College, West Tambaram, Chennai 600 044, India

<sup>1</sup>Research Scholar, Department of Mechanical Engineering, Vels University, Chennai 600 117, India

<sup>2</sup>Department of Mechanical Engineering, Vels University, Chennai 600 117, India

(Received March 28, 2014; Revised June 28, 2014; Accepted August 29, 2014)

**Abstract:** Presently there has been an enormous increase in demand for novel materials to produce complex products with better quality. Hence, plant fibres shall be used to achieve this goal. Hybrid natural fibre composites, can fulfil these requirements. This paper deals with the fabrication and investigation of mechanical properties of hybrid natural fibre composite (banana jute glass fibre) and compares it with single fibre natural composites made up of jute and banana separately. In this work, hand layup method is used to fabricate the composites. The mechanical tests such as tensile, flexural, impact, double shear and delamination tests are performed. Finally, failure morphology analysis is done using Scanning electron microscope (SEM) to know fracture direction, matrix structure and fibre orientation. The results reveal that the hybrid composite has better overall mechanical properties when compared to mono composites containing same materials.

**Keywords:** Mechanical properties, Mechanical testing, Banana jute glass fibre, Hybrid composite, Scanning electron microscope

### Introduction

The present world is facing the challenge to decrease pollution levels while at the same time significantly increasing industrial output. This has led to a number of political initiatives, including support for enhanced industrial use of renewable resources (e.g., biomass, solar, wind power etc) at the expense of non-renewable resources (plastic, glass fibres, etc.). However, plant fibres are now used for industrial purposes to manufacture of new types of materials and products. Zhu and Tobias [1] have provided an insight in techniques for the fabrication of banana-fibre-cement composites and found that physical and mechanical properties of air-cured fibre-reinforced cement composites are high. It was determined that kraft pulped banana fibre, at a loading between 8 and 16 % by mass, resulted in composites with high flexural strength. The result of the investigation of dynamic and static mechanical properties of randomly oriented mixed short banana/sisal hybrid polyester composites and results show that the highest activation energy is found in hybrid composite with volume ratio of banana and sisal as 3:1 [2].

The interfacial adhesion is better in case of epoxy-based composites. Therefore, epoxy is widely used in making natural composites. Kadammi *et al.* [3] studied the use of short palm tree lignocellulosic fibres as reinforcement in polyester and epoxy matrices and to improve interfacial adhesion. The esterification of the lignocellulosic filler in alkaline medium was performed using acetic and maleic anhydrides. Rule of mixtures (ROM) was suggested by Ku

*et al.* [4] who reviewed the tensile properties of natural fibre reinforced polymer composites. Halpin-Tsai equation was used to find the Young's modulus of composites containing different types of natural fibres.

New models and applications of natural fibre composites have been identified to reduce the cost of the existing product. Banana woven fabric reinforcement epoxy composite for household telephone stand and systematic approach of total design process had been presented for better understanding of the best design concept for the product by Sapuan and Maleque [5]. They have also suggested new composites which have better properties over the existing ones. The investigation of acoustical and flammability properties of biodegradable and easily disposable jute fibre and its composite for noise reduction in household appliances, automotive and architectural applications showed that the results characterized low density jute as a better sound absorber as compared to high density jute. Moreover, natural rubber latex jute composite gives higher sound transmission class value than jute felt/cloth [6]. Composite designed through LCA (Life Cycle Analysis) method demonstrate the possibility to use natural fibres through a case design which investigated the environmental improvements related to the replacement of glass fibres for natural jute fibres, to produce a structural frontal bonnet of an off-road vehicle [7] Results showed the suitability of jute fibre composites for Buggy enclosures.

Various mechanical properties such as tensile strength, elongation at break, flexural strength, tensile and flexural modulus of sisal, palm fibre composites have been determined by many researchers [8-12]. Biodegradability of the composites has been evaluated in compost soil burial condition by Behera *et al.* [13]. Fourier transform infra-red (FTIR) and

\*Corresponding author: vijayaramnathb@gmail.com

optical microscope (OM) analyses of the buried samples confirmed the degradation of the composites. El-Tayeb [14,15] used sugarcane fibre (SCF) to develop low cost polymeric composite materials and tested them for mechanical and tribological properties. Nowadays, scanning electron microscope is increasingly used to determine the fibre structure and defects in the composite. Vijaya Ramnath *et al.* [16,22] investigated the mechanical properties of abaca-jute fibre hybrid composite and concluded that hybrid composites have more strength in all aspects as compared to mono composites. Venkateshwaran *et al.* [17] determined the optimum fibre length and morphological analysis using Scanning Electron Microscope. One major disadvantage with most of the natural fibres is that they absorb moisture and weaken as a result. The marine application of glass fibre reinforced polymer composites was studied by Gellert and Turley [18]. Hepworth *et al.* [19] worked on penetration of epoxy resin into plant fibre cell walls increases the stiffness of plant fibre composites and found that epoxy resin can then penetrate into the swollen cell wall and mix with the alcohol and thus increased the stiffness of composites made from flax fibres and epoxy resin. Moreover, the stresses caused in the composite are studied by determining the effects of the composite's constituents on impact properties and post-impact performance is assessed in terms of residual strength [20,21]. An examination on the effects of preform architecture, surface treatment, and z-directional micro-fiber reinforcement on the interlaminar fracture performance of jute/epoxy laminated composites are studied and the result shows that surface treatments increased fracture toughness as a result of improved interfacial adhesion. Unidirectional preforms were found to decrease fracture toughness as compared to plain weave preforms due to reduced inter-ply interaction [23,24].

This paper explores the mechanical properties of natural fibre hybrid composites using banana and jute fibres, fabricated by hand layup method. Various properties of hybrid composite are tested and compared with jute+GFRP and also with banana+GFRP composite. It is found that the hybrid composite has better strength than other composite.

## Experimental

In this paper, hybrid composite is fabricated with banana fibre as a major constituent and jute as a reinforcing agent. The ratio by weight of banana fibre to jute fibre is 7:3. The various materials used in fabrication of the composite by hand layup method are given below:

1. Banana fibre
2. Jute fibre
3. Woven GFRP
4. Epoxy resin (LY 556)
5. Hardener (HY 951)
6. Releasing agent

## Fabrication of the Hybrid Composite

The method used for manufacturing the composite is hand lay method in which all the operations are done manually. Initially the fibres are kept under sunlight to remove moisture content in them. Then, a comb is used to distinctly separate small flakes present in the fibres. A releasing agent (polyvinyl alcohol) is applied on a table for easy removal of the composite. First, two laminates of glass fibre are prepared by coating them with epoxy resin. These laminates of GFRP are allowed to dry for 7 to 10 hours for curing. Once the curing process is complete, the laminate of woven roved GFRP is ready to be used for making the composite samples. Now the releasing agent is applied on the mould and one of the prepared GFRP laminates is placed on it. The resin hardener mixture is applied and the jute fibres are placed vertically parallel to each. Again the resin-hardener mixture is applied over it and then a horizontal layer of banana fibres are laid above the jute layer. Above the layer of banana fibres, a vertical jute layer is laid. The method of applying resin-hardener mixture is repeated after every layer. Once this process is completed the GFRP laminate is laid to form the top surface. Using a separator, the composite material can be easily removed from the mould. Then, a rectangular iron bar of same cross section weighing 25 kg is placed over it. It is kept undisturbed for several hours till the layers and resin mixture dry. The composite is machined according to the required dimension. Hence, the hybrid composite consists of 5 major layers with jute fibres present in 2nd and 4th layer, and banana in 3rd layer. The 1st and the 5th layers are glass fibre reinforced polymer. For jute-GFRP composite the 2nd and 4th layers of banana are replaced by jute fibres in opposite direction. For banana-GFRP composite the 3rd layer is filled with banana fibres laid perpendicular to that of the same in the 2nd and the 4th layer. The volumetric composition of fibres in each layer is one third of the total volume of that layer. The specimen size is 300 mm × 300 mm × 8 mm.

The composites fabricated in this work are named as follows:

Sample 1 = Jute + GFRP

Sample 2 = Banana + GFRP

Sample 3 = Jute + Banana + GFRP

## Testing of Composites

### Tensile Test

Tensile strength is the maximum stress that a material can withstand while being stretched or pulled before failing or breaking. It is customarily measured in units of force per cross-sectional area. The composite after fabrication process is cut as per ASTM: D638 standard using a table saw. A universal testing machine with maximum load rating of 400 kN is used for testing. Three different composite specimens with different fibre combinations namely sample 1, sample 2 and



**Figure 1.** Tensile test specimen after breaking.

sample 3 are tested. The specimen is held in the grip and load is applied until the specimen breaks and the corresponding load and deflections are recorded. Similarly, tensile stress and strain are calculated and load Vs deflection, stress Vs strain graphs are generated. The strength of the composite determined by tensile, flexural, impact and double shear test or a combination of these has a direct influence on the load bearing capacity of the composite and its potential applications. Hence a thorough analysis of the composite is done to determine the overall performance of the composite. The experimental setup is shown in Figure 1.

#### Flexural Test

Flexural strength, also known as modulus of rupture is the strength representing the highest stress experienced within the material at the moment of rupture. In other words, flexural strength introduces tensile stresses in the convex side of the bending specimen and compressive stresses in the concave side, so creating shear stresses over the entire area thus helping to analyse the bending behaviour of specimen. The inner and outer edges of a composite specimen are known as the extreme fibres. The composite is cut as per ASTM: D790 standard. Three different composite specimens namely sample 1, sample 2 and sample 3 are tested. The specimen is held at both ends and load is applied at the centre of the specimen. Flexural stress and strain are calculated and load Vs deflection, stress vs. strain graphs are



**Figure 2.** Flexural testing.

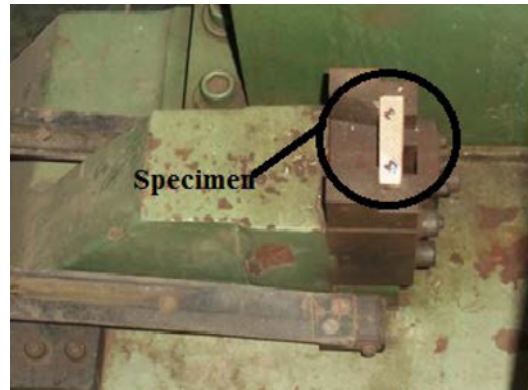


**Figure 3.** Impact test specimen.

generated. Load is applied until the specimen breaks as shown in the Figure 2. The break load and ultimate strengths are noted.

#### Impact Test

Impact strength indicates the ability of a material to withstand a suddenly applied load and it is numerically expressed in terms of energy absorbed in joules. It is mainly performed to determine the service life of the specimen. It is often done with the Charpy impact test apparatus. For a material to have higher impact strength the stresses must be distributed evenly throughout the object. A notched sample is generally used to determine impact energy absorbed by the material. In this work, Charpy impact setup is employed to perform the impact test on the hybrid composite. Here, a pendulum is dropped from an angle of  $135^\circ$  to impact the specimen and to fracture it. The notched specimen is prepared as per ASTM: D256 standard, and it is placed on the arm as shown in Figure 3. The amount of energy absorbed during the breaking of specimen is noted.

#### Double Shear Test

Double shear test is performed using the universal testing machine with a special fixture. The test specimen is prepared



**Figure 4.** Double shear testing.



Figure 5. Delaminated specimen.

as per ASTM: D5379 standard. The specimen is held in the fixture as shown in Figure 4 and the load is applied until the specimen breaks. The breaking load is noted and load vs. deflection graph is generated.

**Inter Delamination Test**

Inter delamination test is performed to know the propagation of crack at the inner surface of the fabricated specimen and also to know the shear strength between successive layers of the composite. The inter-delaminated specimen is shown in Figure 5.

**Results and Discussion**

**Tensile Properties**

The composite specimens namely sample 1, sample 2 and sample 3 are tested for tensile properties in universal testing machine and graphs are drawn for Stress vs. Strain and Load vs. Deflection. The graphs are shown in Figure 6 and 7. Five specimens are tested in each case.

The mechanical properties including break load, maximum deflection, percentage elongation and ultimate tensile strength of the composites are shown in the Table 1. Figure 6

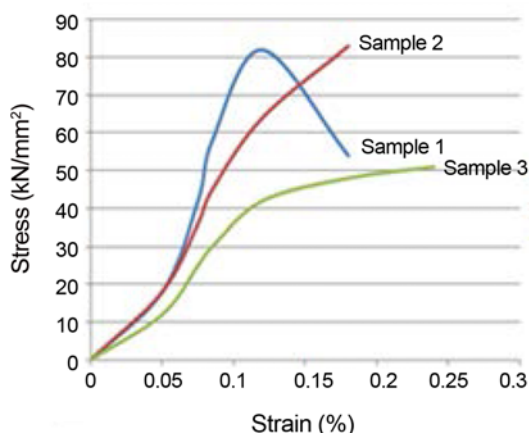


Figure 6. Stress vs strain graph (tensile test).

Table 1. Tensile properties of composites

Composite specimen	Break load (kN)	Maximum displacement (mm)	Elongation (%)	Ultimate tensile strength (MPa)
Sample 1	7.5	6.8	14	51.12
Sample 2	7.95	38	7.6	68.42
Sample 3	9.26	4.6	8.8	85.91

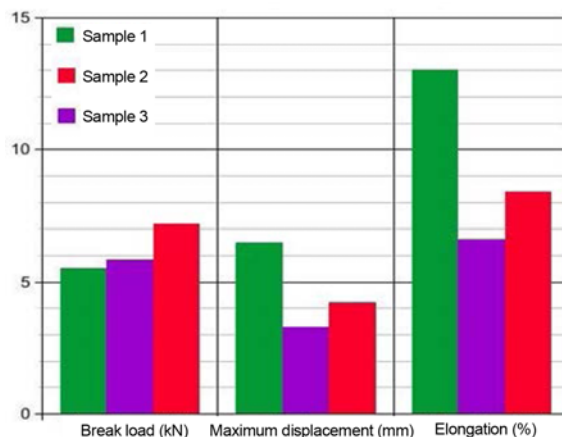


Figure 7. Comparison of break load, maximum deflection, and percentage elongation (tensile test).

shows the stress-strain graph for tensile test performed on the three samples.

It can be seen that almost all the properties of sample 3 are better than that of mono fibre composites. The stress increases linearly with respect to strain for all the composites as shown in Figure 6. But for sample 3 the stress slightly decreases after a particular point, exhibiting ductile properties and this shows the ductility of the material. This is concluded from the fact that the stress-strain curve of a ductile material resembles the graph of sample 3. It is also found that break load and ultimate tensile stress of sample 3 is higher than the other two composites. The percentage elongation of sample 3 is 22.7 % lesser than sample 1. This shows that the former is strained less before failure than the latter. From the tensile test results, it can be concluded that sample 3 has higher strength than other composites. The comparison of break load, maximum deflection and percentage elongation of the three specimens are shown in Figure 7.

Since the sample 3 is a hybrid composite, it is compared with other similar composite from literature as well to get a better understanding of its properties. It can be seen that the sample 3 has ultimate strength of 85.91 MPa which is 40 % greater than abaca-jute-GFRP category I composite [22,26], 54 % greater than category II composite [26] and 22 % greater than category III composite [26]. However, the results obtained from sample 2 and 3 are similar to that obtained by Srinivasan *et al.* [25]. In addition, the tensile test

**Table 2.** Flexural properties of composites

Composite specimen	Flexural break load (kN)	Maximum deflection (mm)	Ultimate flexural strength (MPa)	Flexural modulus (GPa)	Stiffness (N/mm)
Sample 1	0.78	5.8	98.16	1.04	137.73
Sample 2	0.83	6.6	109.86	1.156	125.806
Sample 3	1.02	7.5	151.3	1.233	136.11

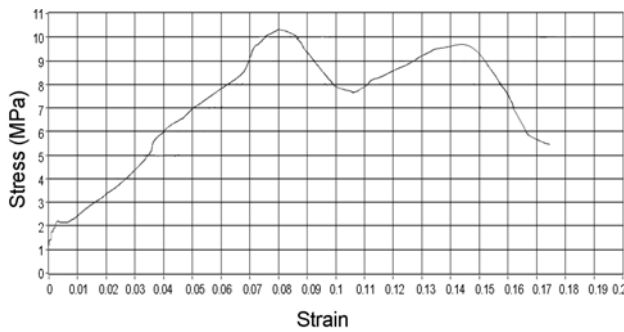


**Figure 8.** Sample graph obtained from UTM for stress vs strain (flexural test).

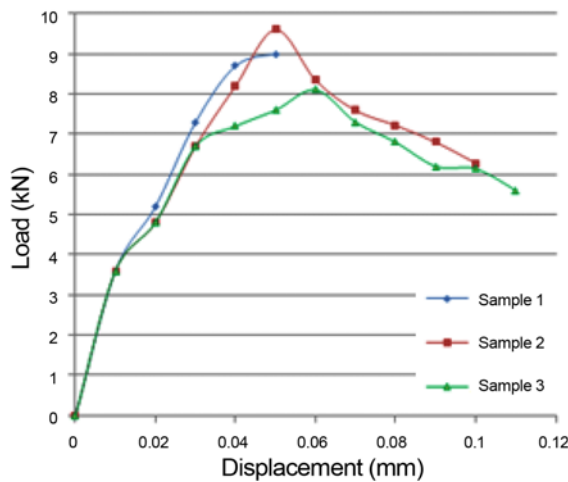


**Figure 9.** Stress vs strain graph (flexural test).

values are seen to be better than that obtained by the Abaca fibre composite [22].

**Flexural Properties**

The flexural properties including break load, maximum displacement, ultimate flexural strength, flexural modulus and stiffness of the three samples are shown in Table 2. It can be seen that almost all the properties of sample 3 are higher than the others. A typical stress-strain curve obtained from the UTM for flexural test is shown in the Figure 8. Figure 9 shows the stress-strain graph of flexural test performed on the three samples.

From Figure 9 it can be seen that, the stress-strain curve for sample 1 and sample 2 increases linearly up to ultimate

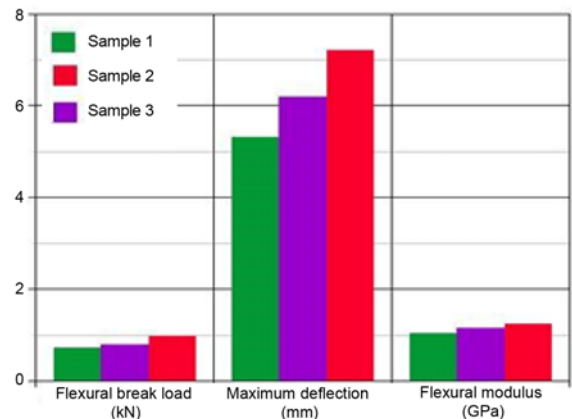


**Figure 10.** Comparison of flexural break load, maximum deflection, and flexural modulus.

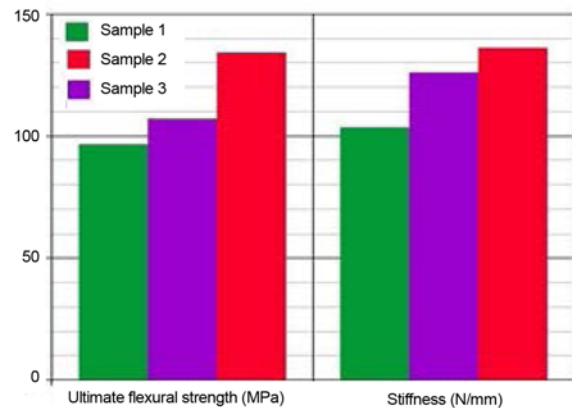


**Figure 11.** Comparison of ultimate flexural strength and stiffness of composites.

flexural stress and then decreases due to breakage. sample 3 has more flexural strength than the other composites.

The flexural modulus of the composites is found at the linear portion of the load-displacement curve. The flexural break load of sample 3 is 1.34 times that of sample 1 and 1.25 times the flexural break load of sample 2. Beyond the maximum flexural load point, the graph decreases and shows haphazard behaviour since the fibres tend to pull out from the composite at the breaking point. This leads to the fluctuations in the curve until it breaks. From Figure 10 it is clear that the maximum displacement is higher for sample 3 since the hybrid composites containing banana and jute

fibres bear more load than individual composites. Figure 11 shows that the stiffness and flexural strength of sample 3 are higher than the others.

Similar to the tensile test, the flexural test is also compared to the literature to get an overall perspective. It is found that flexural test result of sample 2 is in order with that found out by Venkateshwaran *et al.* [17]. But the sample 3 shows far more superior load bearing capacity. It has a break load of 1.02 kN which is 1.26 times greater than the average break load for the abaca-jute-GFRP composite [26]. It is almost equal to the values found by Srinivasan *et al.* [25].

**Impact Properties**

The energy absorbed by the specimens during impact test is furnished in Table 3. It is found that sample 1 and sample 2 absorb less energy than sample 3. The reason for this is that the hybrid composites have dual type of fibre arrangement throughout the matrix. It is difficult for cracks to propagate, when the layers are of different type of fibre in alternate directions. Thus, energy absorption capacity of the sample 3 is higher when compared to the other two samples. Figure 12 shows the comparison between energy absorbed and the impact strength of three composites.

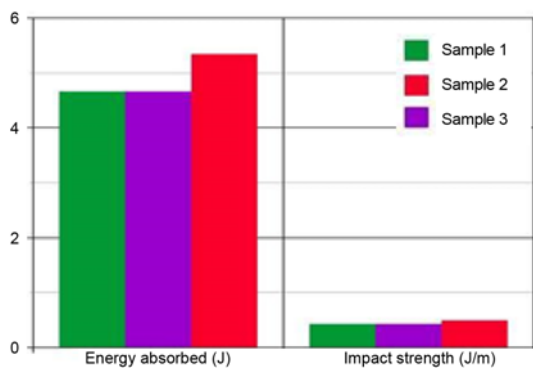
When the results obtained in Flexural test are compared with literature, the values are found to be in accordance and there is not much variation between the three samples in this work and those values obtained from Vijaya Ramnath *et al.* [26].

**Double Shear Properties**

The results of double shear test are shown in Table 4.

**Table 3.** Impact properties of composites

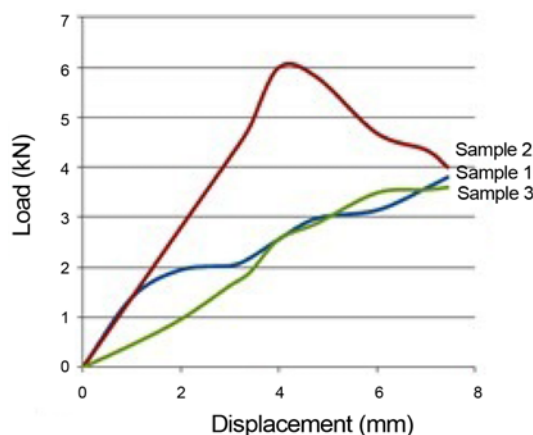
Composite specimen	Energy absorbed (J)	Impact strength (J/m)
GFRP+Banana	4.66	423.63
GFRP+Jute	4.66	423.63
GFRP+Jute+Banana	5.33	484.54



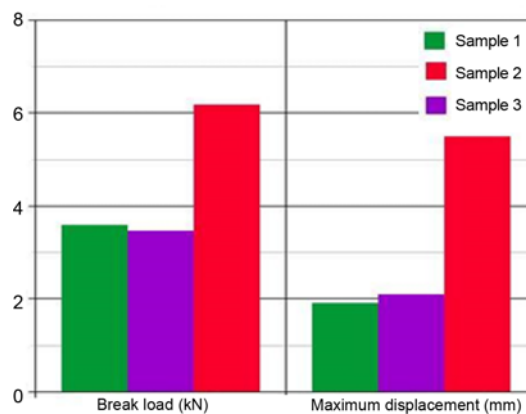
**Figure 12.** Comparison between energy absorbed and impact strength of composites.

**Table 4.** Double shear properties

Composite specimen	Break load (kN)	Maximum displacement (mm)	Ultimate shear strength (MPa)
Sample 1	3.595	1.9	52.0
Sample 2	3.465	2.1	54.0
Sample 3	6.180	5.5	64.0



**Figure 13.** Load vs displacement graph for double shear test.



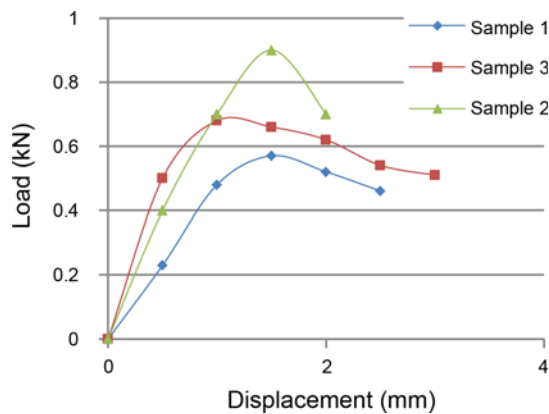
**Figure 14.** Comparison between break load and deflection of composites.

Figure 13 shows the load-displacement graph for double shear test performed on three samples. It shows that the displacement increases linearly as the load increases, and then there is a small dip in the curve. This small dip in graph corresponds to yield load. The break load for sample 3 is much higher than the other two composites. The comparison between different composites for double shear test is shown in Figure 14 which shows that the maximum displacement is higher for sample 3 than sample 1 and sample 2 since it bears more load than the latter. The ultimate shear strength of sample 3 is 1.23 times higher than sample 2 and 1.18 times higher than sample 2.

Compared to literature [16], the double shear properties of

**Table 5.** Delamination properties of composites

Composite specimen	Break load (kN)	Maximum displacement (mm)	Ultimate strength (GPa)
Sample 1	0.68	3.1	0.0471
Sample 2	0.81	4.2	0.0521
Sample 3	0.94	2.2	0.0907

**Figure 15.** Load vs displacement graph for inter delamination test.

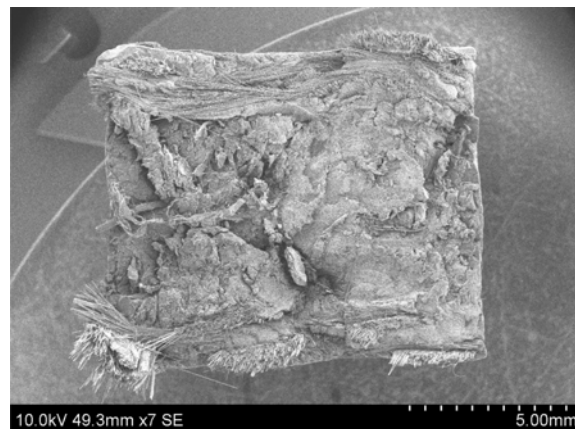
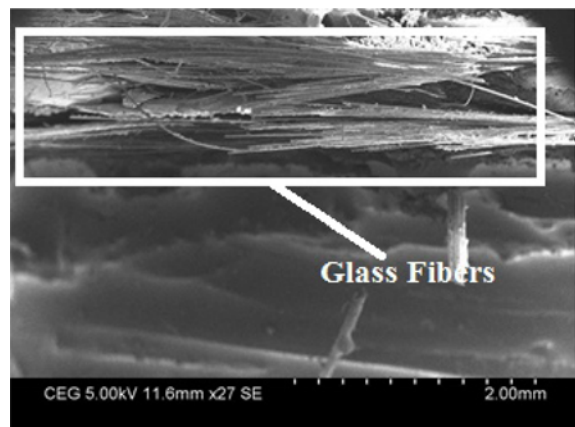
all the three samples are lower. This may be attributed to variation in the arrangement of layers of composite. Twinned fibers are known to produce better properties.

### Inter Delamination Properties

Delamination is one of the modes of failure in composite materials. It occurs in laminated materials like composites due to fatigue and cyclic stresses. The break load, maximum displacement and ultimate strength are shown in Table 5. From the table, it can be seen that almost all the properties of sample 3 are higher than the other two mono composites. A typical load-displacement curve is shown in the Figure 15. From this figure, it can be seen that the load-displacement curve for all the composites increase linearly with respect to displacement up to the maximum load and then decreases due to fracture. After the maximum load point the graph decreases since the fibres tends to pull out from the composite at the breaking point. The maximum displacement is higher for sample 3 since it bears more load than sample 2 and sample 1. From the literature results, it can be inferred that all the three samples have better results when compared with the samples in literature [23].

### Morphological Analysis

Morphological analysis is done using a SEM as shown in Figure 16. The internal surface characteristics of the composite material are studied through SEM after conducting tests. The samples are taken from each test, dried and coated with 15-20 nm thick layer of gold with an ion-sputter coater device. Subsequently the specimens are inspected by a scanning electron microscope. The interfacial

**Figure 16.** SEM setup.**Figure 17.** Cross section of sample 3 before various tests.**Figure 18.** SEM image of sample 3 after impact test.

adhesion between matrix and the fibre is clearly seen from scanning electron micrographs.

The SEM image of sample 3 is shown in Figure 17. It indicates the cross section of the composite before the various mechanical tests are performed. It is used as a base image to compare the cross section of the composite with the same composite after it has undergone the mechanical tests.



**Figure 19.** SEM image of sample 3 after tensile test.

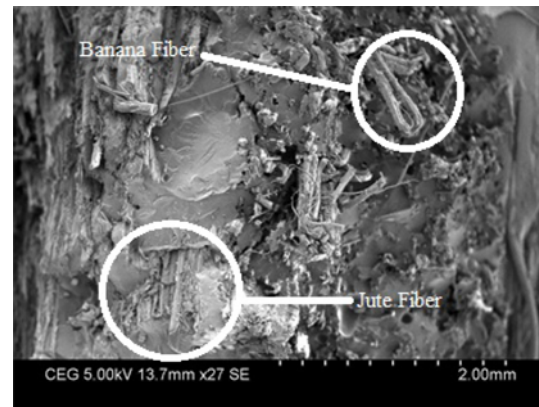


**Figure 21.** SEM image of sample 3 after flexural test.

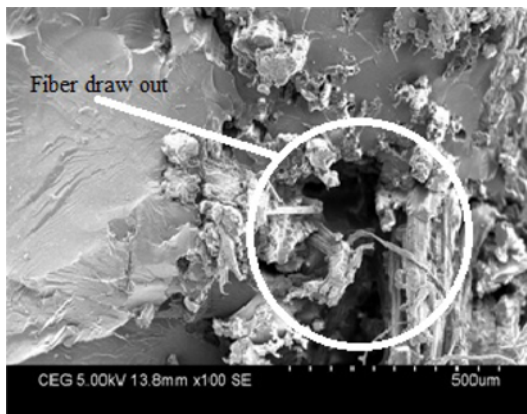


**Figure 20.** SEM image of sample 3 after double shear test.

It can be seen that a uniform layer of natural and glass fibers are present with the resin providing the bonding needed to hold them together.

The SEM micrograph of the sample 3 after impact test is shown in Figure 18. The fibres are fractured due to the sudden impact which is clearly seen in the image. Moreover, due to the woven nature of the glass fibre, it is clear that there is a uniform distribution in the matrix and interfacial adhesion is also present up to a nominal level. When compared with Figure 17, it is evident that glass fibers break before the natural fibres which eventually lead to the total failure of the composite.

Figure 19 shows the arrangement of fibres in the composite. The top portion of the image shows the banana fibres in horizontal direction and the centre part shows the fibre in vertical direction. Since the loading for tensile test is done in horizontal direction, the fibres are found to be damaged in that direction more than in the other direction unlike in impact test where the glass fibers break simultaneously. Moreover, compared to Figure 17, the fibers break in an uneven manner.

Figure 20 shows the SEM micrograph of sample 3

composite after double shear test. The adhesion between the fibres and resin is clearly seen in the micrograph. On the contrary there are few defects like air bubbles and fibre draw-out due to improper fabrication. A comparison with the base image shows the missing fibre in the composite. Figure 21 shows the SEM micrograph of a flexural fractured specimen. Interphase delamination is found at the cross-section of a composite due to flexural load applied. Presence of voids in the specimen is found to be minimal due to uniform load applied on it.

## Conclusion

This paper shows the hand layup method of fabricating hybrid natural composite using Jute and Banana with Glass fibre and comparing their mechanical properties. From the tests results, the following conclusions are drawn:

1. The ultimate tensile strength of the sample 3 is  $83.74 \text{ N/mm}^2$  which is higher than that of sample 1 with  $66.35 \text{ N/mm}^2$  and sample 2 with  $49.31 \text{ N/mm}^2$ .
2. The percentage elongation of sample 3 is higher than the percentage elongation of the sample 2 but lesser than sample 1 under tensile loading.
3. The sample 3 excels well under flexural test, yielding flexural stiffness of  $136.11 \text{ N/mm}^2$  and ultimate flexural strength of  $134.05 \text{ N/mm}^2$ , which is higher than that of the other samples.
4. Sample 3 exhibits higher impact resistance and it absorbs  $5.33 \text{ J}$  against  $4.66 \text{ J}$  of sample 1 and sample 2.
5. The ultimate shear strength of sample 3 ( $64 \text{ N/mm}^2$ ) is comparatively higher than  $71.1 \text{ N/mm}^2$  of sample 2.
6. Hybridizing also favours in inter de-lamination test which shows the breaking load increasing from  $0.81 \text{ kN}$  to  $0.94 \text{ kN}$  for sample 3.

SEM images of the tested specimens helps to predict the defects, voids, crack propagation and resin distribution and aides in better understanding of the composite.



## References

1. W. H. Zhu and B. C. Tobias, *Cem. Concr. Compos.*, **16**, 3 (1994).
2. M. Idracula, S. K. Malhotra, K. Joseph, and S. Thomas, *Compos. Sci. Technol.*, **65**, 1077 (2005).
3. A. Sbiai, A. Maazouz, E. Fleury, H. Sautereau, and H. Kaddami, *Bioresources*, **5**, 672 (2010).
4. H. Ku, H. Wang, N. Pattarachaiyakoo, and M. Trada, *Compos. Pt. B-Eng.*, **42**, 856 (2011).
5. S. M. Sapuan and M. A. Maleque, *Mater. Des.*, **26**, 65 (2005).
6. S. Fatima and A. R. Mohanty, *Acoustics*, **72**, 108 (2011).
7. C. Alves, A. Silva, L. Reis, P. Ferrão, and M. Freitas, "New Trends and Developments in Automotive Industry", 1st ed., p.12, InTech, 2011.
8. K. Hamid, D. Alain, K. Bertine, B. Abdelkader, T. Moha, and R. Mustapha, *Compos. Pt. A-Appl. Sci. Manuf.*, **37**, 1413 (2006).
9. D. D. R. Cartie and P. E. Irving, *Compos. Pt. A-Appl. Sci. Manuf.*, **33**, 483 (2002).
10. M. Iricula, S. K. Malhotra, K. Joseph, and S. Thomas, *Compos. Sci. Technol.*, **65**, 1077 (2005).
11. C. Pavithran, P. C. Mukherjee, M. Brahma Kumar, and A. D. Damodarn, *J. Mater. Sci.*, **26**, 455 (1991).
12. B. F. Yousif and H. Ku, *Mater. Des.*, **36**, 847 (2012).
13. S. Avancha, A. K. Behera, R. Sen, and B. Adhikari, *J. Appl. Polym. Sci.*, **127**, 4861 (2013).
14. N. S. M. El-Tayeb, *Wear*, **265**, 223 (2008).
15. N. S. M. El-Tayeb, *Mater. Des.*, **30**, 1151 (2008).
16. B. Vijaya Ramnath, S. Junaid Kokan, R. Niranjana Raja, R. Sathyanarayanan, C. Elanchezhian, A. Rajendra Prasad, and V. M. Manickavasagam, *Mater. Des.*, **51**, 357 (2013).
17. N. Venkateshwaran, A. Elayaperumal, A. Alavudeen, and M. Thiruchitrambalam, *Mater. Des.*, **32**, 4017 (2011).
18. E. P. Gellert and D. M. Turley, *Compos. Pt. A-Appl. Sci. Manuf.*, **30**, 1259 (1999).
19. D. G. Hepworth, J. F. V. Vincent, G. Jeronimidis, and D. M. Bruce, *Compos. Pt. A-Appl. Sci. Manuf.*, **31**, 599 (2000).
20. J. K. Chen and C. T. Sun, *Compos. Struct.*, **4**, 59 (1985).
21. M. O. W. Richardson and M. J. Wisheart, *Compos. Pt. A-Appl. Sci. Manuf.*, **27**, 1123 (1996).
22. R. Niranjana Raja, S. Junaid Kokan, R. Sathya Narayanan, S. Rajesh, V. M. Manickavasagam, and B. Vijaya Ramnath, *Adv. Mat. Res.*, **718-720**, 63 (2013).
23. B. Vijaya Ramnath, C. Elanchezhian, P. V. Nirmal, G. Prem Kumar, V. Santhosh Kumar, S. Karthick, S. Rajesh, and K. Suresh, *Fiber. Polym.*, **15**, 1251 (2014).
24. A. M. Pinto, B. V. Chalivendra, K. Y. Kim, and F. A. Lewis, *Eng. Fract. Mech.*, **114**, 104 (2013).
25. V. S. Srinivasan, S. RajendraBoopathy, D. Sangeetha, and B. Vijaya Ramnath, *Mater. Des.*, **60**, 643 (2014).
26. B. Vijaya Ramnath, V. M. Manickavasagam, C. Elanchezhian, C. Vinodh Krishna, S. Karthik, and K. Saravanan, *Mater. Des.*, **60**, 620 (2014).